

2 Scientific Performance

The LZ detector system described in the previous and subsequent chapters is highly sensitive to a variety of physics signals. The principal signal we seek is that of NRs distributed uniformly throughout the LXe TPC volume, in response to an impinging flux of nonrelativistic WIMPs that are gravitationally bound to the Milky Way galaxy. In the first sections of this chapter, we describe the sensitivity to various WIMP-particle cross sections.

The first step in selecting the sample of WIMP candidates is to define a search region in the two variables: S1 (the prompt scintillation light) and S2 (the delayed electroluminescence light, a measure of primary ionization). The use of both variables allows the distinction of NRs from the much more numerous ERs.

The LUX collaboration has recently completed extensive calibrations of the response of liquid xenon to NRs [1] and ERs [2], as shown in Figure 1.3.11. These high-statistics data permit us to employ the detailed shapes of the response probability distribution functions (PDFs) in a profile likelihood ratio (PLR) fit to estimate the LZ sensitivity to NRs from WIMPs.

We first describe our sensitivity and discovery potential for the spin-independent (SI) WIMP-nucleon interaction. We then discuss interpretations involving more general forms of the WIMP-nucleon interaction.

Should LZ see a WIMP signal, the distribution of that signal in NR energy will allow constraints on the WIMP-Xe scattering cross section, the WIMP-Xe reduced mass, and on the velocity distribution of galactic WIMPs [3].

A variety of other physics processes can be probed by selective detection of NRs and ERs as defined with S1 and S2. The central fiducial region of the LZ detector will be an extraordinarily quiet laboratory for processes that deposit energy. Among the physics processes that can be probed are:

1. Solar neutrino detection.
2. A neutrino magnetic moment.
3. Double beta decay.
4. Neutrinos from supernovae.
5. Sterile neutrinos.
6. Interaction of WIMPs with atomic electrons.
7. Solar and certain dark-matter axion-like particles (ALPs).
8. Exotic particles that interact in the LZ outer detector.

2.1 WIMP Sensitivity and Discovery Potential

The principal physics analyses of the LZ experiment will be searches for the recoils of Xe atoms caused by the interaction of WIMPs with the Xe nucleus. As discussed above, two types of signal are formed in the LXe response to the recoils: S1 and S2. In the principal LZ search, the energy of the recoil is reconstructed from a combination of S1 and S2, and the ratio S2/S1 provides discrimination of NRs from the background of ERs. The value of the reconstructed energy depends on whether the event is an NR or an ER.

2.1.1 S1+S2 Analysis

The S1+S2 analysis in LZ will follow the general framework of the recently published LUX search for NRs in response to WIMPs [4, 5]. We define a search region in the plane of $\log_{10}(S2)$ versus S1, shown in Figure 2.1.1.¹ LUX determines the sensitivity to WIMP-nucleon scattering with a multi-dimensional PLR fit in that plane, which is also how the LZ sensitivity is determined.

A comparison of the key performance assumptions for LZ as well as the comparable achievements in LUX are given in Table 2.1.1. The baseline detector performance assumed for LZ is in many aspects more conservative than that achieved by LUX. The most prominent exception in Table 2.1.1 is the liquid/gas emission probability, where we presume that the limitations of the LUX electric field will be removed in the LZ experiment.

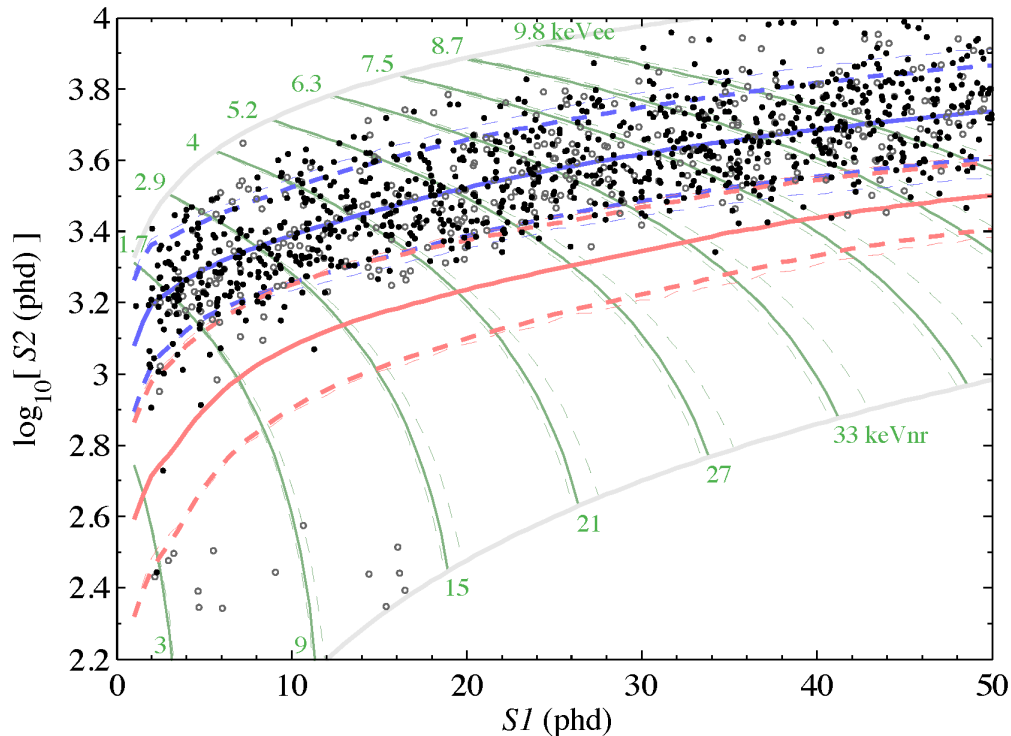


Figure 2.1.1: The LUX WIMP search data [5]. Shown is all data after selection criteria for the 332 live days of the LUX 2014-2016 run. The logarithm of S2 is plotted versus S1, after spatial corrections. Filled black circles are in the detector central region (radius <18 cm) and the edge of the detector (radius 18 cm to 20 cm) in grey open circles. The centroid (solid) and search region boundaries (dotted) are red for the signal (NR) region or “band”, and corresponding lines in blue describe the primary background (ER) band. The dotted lines are $\pm 1.28\sigma$ around the centroid. Contours of equal recoil energy for NR (keV_{nr}) and ER (keV_{ee}) interpretations are shown in grey. The unit “phd” is photons detected, and results from correcting the photoelectrons detected for the probability of one UV photon inducing two photoelectrons. The data is consistent with a background of ERs and wall-induced events.

The benchmark process we will use to interpret NRs will be the interaction of WIMPs via an SI process, such as exchange of a Higgs particle [6], with the gluons in the nucleons in the Xe nucleus [7]. This process produces a WIMP-nucleus scattering rate that is independent of the identity, neutron or proton, of the nucleon

¹Sometimes, the equivalent plane of $\log_{10}(S2/S1)$ versus S1 is utilized to display the same data.

Table 2.1.1: Key LZ and LUX Assumptions Compared

Quantity	Units	LZ Assumption	LUX [5]
Recoil threshold, 50 % efficiency	keV _{nr}	6	3.3
S1 range	Photons detected	3 – 30	2 – 50
S2 range	Photons detected	>350	>200
S1 light-collection efficiency	Absolute	7.5 %	14 %
Photocathode efficiency	Absolute	25 %	30 %
Liquid/gas emission probability	Absolute	95 %	73 %
ER discrimination	Absolute	99.5 %	99.8 %

in the nucleus. For the low-momentum transfers of typical WIMP interactions, the scattering amplitude is proportional to A , the number of nucleons in the nucleus. The scattering cross section includes the density of states, which also favors larger A , while the threshold for energy detection favors smaller A . The nuclear form factor is employed to account for quantum-mechanical interference attributable to the non-zero nuclear size [8], and the standard halo model (SHM) of the distribution of WIMP velocities in the Milky Way is used [9].

The backgrounds expected for LZ are described in detail in Chapter 9 and summarized in Table 1.6.1 and in Table 12.3.1. In the LZ Conceptual Design Report (CDR) [10], we performed a simple cut-and-count estimate of the LZ sensitivity, under the assumption that 0.5 % of the ER events would contaminate an NR signal region defined to retain 50 % of NR events. The vastly improved understanding of the PDFs of ERs and NRs in S1 and S2 achieved by LUX have caused us to utilize the more advanced PLR statistical technique for estimates of WIMP sensitivity in this report[11]. In general this technique substantially reduces the fraction of ER events that contaminate the NR signal region, as discussed in Section 12.3.1. A consequence is the extremely stringent requirements in the LZ CDR on the permissible rate of radon decays in liquid xenon are substantially relaxed in this report, to a level of ≈ 20 mBq for the 10 tonnes LZ total volume. This rate of radon decays is commensurate with the achievements of LUX and other existing liquid xenon experiments. However, at a radon decay rate of ≈ 20 mBq ERs from the quiet beta decays of radon daughters outnumber ERs from solar pp neutrinos by a factor of about 3.5.

The resulting sensitivity plot is shown in Figure 2.1.2, along with LUX and ZEPLIN limits. For the baseline assumptions described in this report, LZ achieves a median sensitivity at a mass of approximately $40 \text{ GeV}/c^2$ of $2.3 \times 10^{-48} \text{ cm}^2$.

The project LZ sensitivity for low WIMP masses is considerably improved in this report, compared to the CDR. The improvement is due to the utilization in this report of the improved calibrations reported by LUX[1, 2], which document higher S1 and S2 responses to low energy NR than were assumed in the CDR. Further improvements in sensitivity for low WIMP masses is possible through an ‘‘S2-only’’ analysis[12], or through the detection of bremsstrahlung from the nuclear recoil[13].

2.2 Neutrino Physics

The LZ detector will have a sufficiently large mass and low background that several types of neutrino interactions will be visible. These events will be uniform throughout the liquid xenon volume and cannot be shielded. We have studied the sensitivity of LZ to solar, atmospheric, astrophysical, reactor, and geophys-

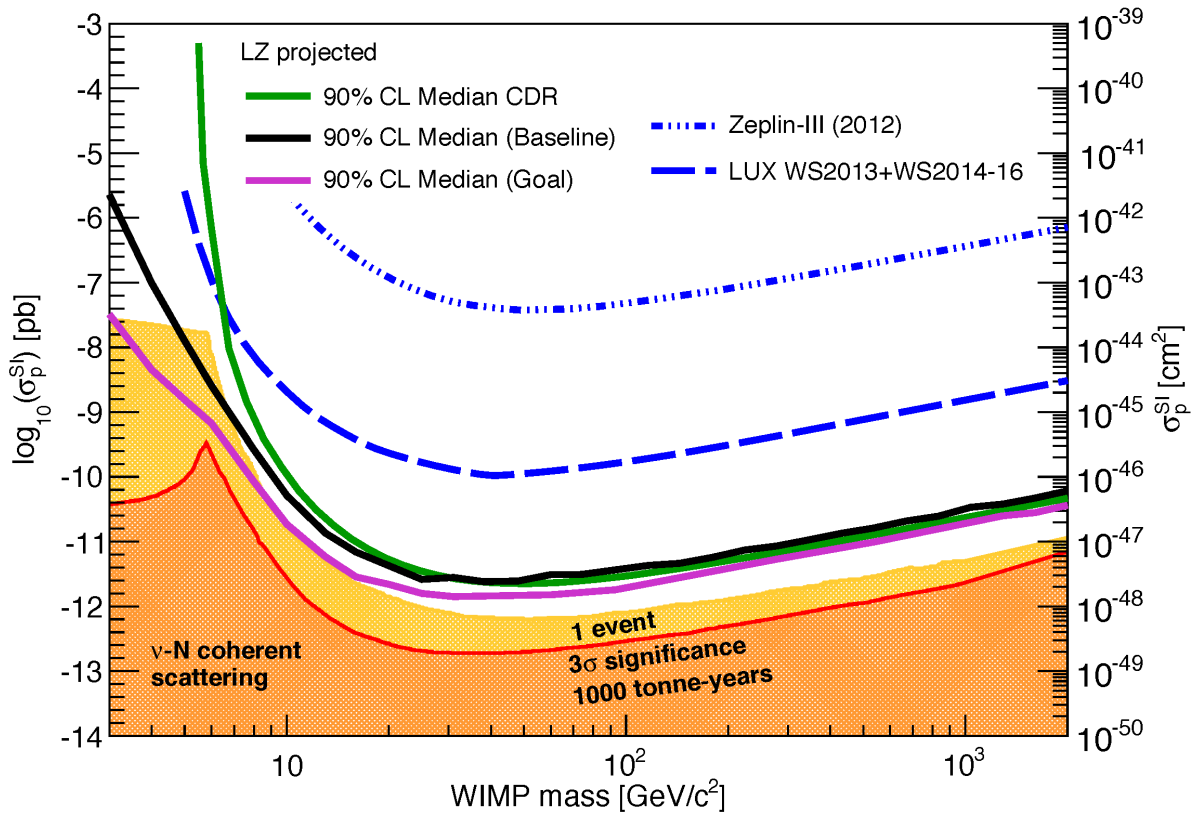


Figure 2.1.2: LZ sensitivity projections. The baseline LZ assumptions described in this Technical Design Report give the solid black curve. LUX and ZEPLIN results are shown in broken blue lines. If LZ achieves the design goals listed in Table 12.3.2, the sensitivity would improve, resulting in the pink sensitivity curve. The gray line shows the projected sensitivity in the LZ Conceptual Design Report (CDR) [10] (see text for details of the changes from the CDR to this report). The shaded regions show regions where background NRs from cosmic neutrinos emerge [14].

ical neutrinos. In particular, solar neutrinos have been considered as both an interesting signal and as an irreducible background to a WIMP search.

LZ will observe the pp fusion chain of our sun in real time via elastic $\nu e \rightarrow \nu e$ scattering, in a lower energy regime than the only other real-time measurement to date, and will most likely detect neutrinos from ^8B via coherent nuclear scattering. The coherent neutrino signal from a nearby supernova would be a unique, flavor-independent probe of the neutrino flux.

We have also estimated the potential of LZ to observe neutrinoless double-beta decay ($0\nu\beta\beta$) from ^{136}Xe , and considered the impact on the reactor/source neutrino anomaly and on searches for a neutrino magnetic moment of a prolonged exposure of LZ to a nearby ^{51}Cr neutrino source.

2.2.1 Solar and Atmospheric Neutrinos

2.2.1.1 Elastic Scattering of Solar Neutrinos

A prominent background for WIMP dark matter searches in LZ will come from the elastic scattering of solar neutrinos from the pp fusion chain [15] with the atomic electrons in xenon. Our calculations of the rate of these scatters agree with those of [16] under the same assumptions. The calculations in this report, however,

use updated neutrino mixing parameters [17] and solar fluxes obtained from a luminosity-constrained analysis of Borexino data (cf. Table 2 of [18]). Our projections assume the standard LZ fiducial target mass of 5.6 tonnes and an exposure of 1,000 live days. For electron recoil events with energies between 1.5 and 20 keV_{ee}, we expect 838 observable pp events, 69 events from ⁷Be and <10 events from ¹³N. For electron recoil energies above 20 keV_{ee}, 2νββ events from ¹³⁶Xe are expected to dominate the counting rate.

In the WIMP dark matter search window between 1.5 and 6.5 keV_{ee}, the corresponding calculated numbers are 233, 19 and 3 for a total of 255 electron recoil background events from solar neutrinos. Our calculation has neglected atomic binding effects on the scattering process. Inclusion these effects will result in a suppression of result in a suppression of 24 % to 28 % [19].

The LZ experiment would add an interesting data point to the existing world experimental sample on pp solar neutrinos, in the context of the MSW-LMA explanation to the observed solar neutrino flux. Existing data to support this model in the low-energy regime are from the SAGE experiment [20] and from Borexino [21]. The 50 tonnes gallium target in SAGE inferred 854 inverse beta decay events attributed to pp solar neutrinos over 18 years of operations. The neutrino energy threshold for that measurement was 233 keV. More recently, the Borexino Collaboration made the first real-time detection of the pp solar neutrinos via the elastic scattering process with atomic electrons. The Borexino neutrino energy threshold was ≈300 keV, while LZ will be uniquely sensitive, with a neutrino energy threshold of a few tens of keV.

Although the LZ experiment will open up new experimental territory in the study of pp solar neutrinos, the current consensus in the solar neutrino community is that the accuracy of an pp solar neutrino measurement must be better than 1 % to improve understanding of solar neutrinos [18]. To achieve 1 % accuracy, LZ would need to observe several tens of thousands of pp neutrino-induced ER events, and also control systematics at a sub-1 % level. The elimination of the ¹³⁶Xe isotope and a live time of 2,000 to 4,000 days would allow the accuracy of an LZ measurement of pp solar neutrinos to approach 1 %.

2.2.1.2 Coherent Nuclear Scattering of Solar Neutrinos

Neutrinos are expected to elastically scatter coherently across nucleons in the nucleus [22, 23]. This process has yet to be observed. Dedicated experiments aim to measure the process in the laboratory. The energy transferred to the nucleus from coherent neutrino scattering is typically suppressed by $\approx m_e/m_N$ relative to the elastic electron scattering process, so signals from the coherent scattering of solar pp neutrinos will fall well below the LZ S1+S2 detection threshold.

Neutrinos from ⁸B decay, which occur at the end of the pp chain about 0.1% of the time, range in energy up to ≈15 MeV. This energy is sufficient to transfer up to a few keV of energy to a xenon nucleus via coherent scatter, and so these events are expected to fall at the threshold of detectability in LZ. Figure 2.2.1 (left) shows the expected rate and signal distribution of these events. Our calculations agree with those of [24] if we make the same assumptions. For the calculations in this report, we assume a ⁸B neutrino flux of $5.25 \times 10^{-6} \text{ cm}^{-2} \text{ s}^{-1}$ as measured by SNO [25], with a total uncertainty of <5 %. The largest uncertainty in the number of detected ⁸B neutrinos is due to the signal yield in the liquid xenon. We assume the latest results obtained by the LUX Collaboration [4]. Assuming LZ baseline detector parameters we expect 7 events from ⁸B coherent neutrino scatter in the full 5,600 tonne-day LZ exposure. Systematic uncertainty, due primarily to photon collection and liquid xenon signal yields) is comparable to statistical uncertainty in this case.

The measurement of the flux of ⁸B neutrinos through coherent neutrino scattering is sensitive to all neutrino flavors, forming an interesting result in its own right. From a dark matter perspective, these neutrinos are an irreducible background which looks very similar to a 6 GeV WIMP. The distinct and complimentary calibrations planned in LZ, described in Chapter 7 will allow a thorough mapping of the ⁸B neutrino signal region. Combined with the distinctive, soft spectrum of ⁸B neutrino events, LZ will be able to in essence fit and subtract out the ⁸B neutrinos from the WIMP search.

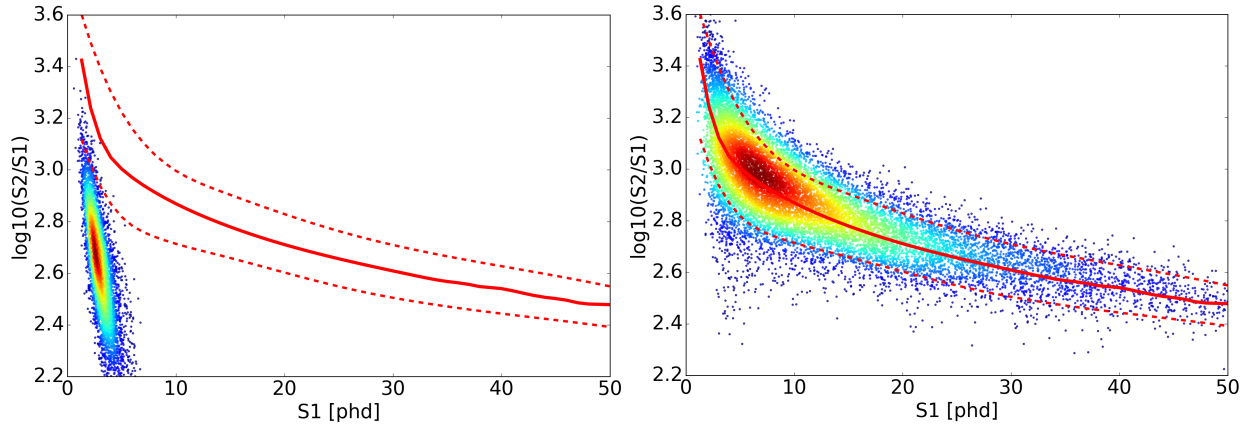


Figure 2.2.1: Calculated high-statistics probability distribution functions (PDFs) for ${}^8\text{B}$ (left panel) and atmospheric (right panel) coherent neutrino-nucleus scattering events. The solid curve is the centroid of the nuclear recoil band, and the dotted lines define a $\pm 3\sigma$ band. These lines are defined for a spectrum *flat* in nuclear recoil energy. The recoils from ${}^8\text{B}$ on the left fall outside the band because the bulk of the PDF is under the threshold, and correlated fluctuations must occur for events to enter this plot. In 5,600 tonne-day of LZ exposure, we expect a mean of 7 and 0.5 NR events from these neutrino sources to meet selection requirements.

In contrast to the atmospheric neutrino signal (Fig. 2.2.1, right panel), the ${}^8\text{B}$ signal shown (Fig. 2.2.1, left panel) appears below the nuclear recoil band. This is true despite the fact that both distributions are due to nuclear recoils from coherent neutrino nucleus scattering. The primary reason is an artifact of the signal detection threshold. Because LZ will not be able to detect fewer than one S1-induced detected photon, the ${}^8\text{B}$ signal consists of the tail of upward fluctuations in the number of scintillation photons produced. This comes at the expense of the number of ionized electrons in the S2 signal. Therefore, the ratio S2/S1 for these events is systematically biased below the nuclear recoil band, which is defined for a *flat* distribution in recoil energy.

2.2.1.3 Atmospheric Neutrinos

Atmospheric neutrinos result from muon and pion decay in the atmosphere. Historically, they were considered as a background for nucleon decay experiments, and then exhibited a surprising flavor-mixing phenomenon that has now been verified in accelerator-based experiments.

Consequently, the literature shows measurements or calculations of the atmospheric neutrino flux for energies $\gtrsim 1$ GeV. The flux of atmospheric neutrinos is not a significant background for LZ in the elastic neutrino-electron scattering channel. However, coherent neutrino-nucleus scattering events present a serious background concern. This is because the hard energy spectrum of the neutrinos results in a recoil spectrum which is essentially indistinguishable from a typical WIMP. The PDF for the expected spectrum is shown in Figure 2.2.1 (right).

There is a detector-dependent sweet spot in neutrino energy for detection of coherent neutrino nucleus scattering. For LZ this is in the range of a few tens of MeV. Lower energies cannot register a signal, and higher energies begin to suffer a nuclear form factor suppression from the loss of coherence. Therefore LZ is singular in its need to understand the atmospheric neutrino flux for energies $\lesssim 100$ MeV. A single calculation exists for the flux in this energy region [26], and it is tailored to two particular experimental sites: Kamioka, and Gran Sasso. The latitude of the site is important because the largest uncertainty is attributed to the

geomagnetic cutoff, which limits the penetration of the primary cosmic rays into the atmosphere. Previous work [24] assumed the flux values for Kamioka, which are about 30 % lower than the flux at Gran Sasso.

Our event rate calculations assume the Gran Sasso flux values tabulated in [26], with a single-sided uncertainty of 50 %. This uncertainty was estimated by comparing the Kamioka, Gran Sasso and SURF locations with a vertical cutoff rigidity map [27]. In 5,600 tonne-days, LZ expects to observe 0.5 signal-like events from atmospheric neutrinos, distributed in S2 and S1 very much like the expected signal from a high-mass WIMP. This PDF shown in Fig. 2.2.1 (right panel).

2.2.1.4 Neutrino Magnetic Moment

It is not known if the neutrino has a small magnetic moment, and upper limits exist on its possible magnitude. The strongest direct particle physics upper limit is $5.4 \times 10^{-11} \mu_B$ from Borexino [28], while analysis of supernovae provide a stronger upper limit of $5 \times 10^{-13} \mu_B$ [29].

The effect of a neutrino magnetic moment is an increased scattering rate with electrons. A larger magnetic moment shifts the turn-on of the increase to higher energy. The ≈ 1 keV energy threshold of LZ suggests an order of magnitude improvement in sensitivity, relative to Borexino. This is shown in Fig. 2.2.2, assuming $\mu_\nu = 5 \times 10^{-12} \mu_B$, in which case an increase in the scattering rate at threshold would be just barely observable.

2.2.1.5 Other Neutrino Backgrounds

One other possible source of signal-like events arises from coherent neutrino-nucleus scattering of the diffuse supernova neutrino background (DSNB). We estimate this background in the NR search region to be 0.05 (DSNB)

for the LZ fiducial mass of 5.6 tonnes and run duration of 1,000 days.

Geophysical neutrinos from ^{238}U and ^{232}Th decays have been seen by the KamLAND [30–32] and Borexino [33] detectors. Those detectors have an energy threshold for neutrinos of about 1.8 MeV. They are unable to detect neutrinos from the decay of ^{40}K , which have an energy just below 1.5 MeV. Using the Reference Earth Model and neutrino flux calculations from the KamLAND work, we estimate for LZ 1.5 ER events/year from ^{40}K decay, 0.3 ER events/year from ^{238}U decay, and 0.2 ER events/year from ^{232}Th decay. With the ability to distinguish ER and NR in LZ, these signals provide negligible backgrounds for the dark-matter search.

It is possible for neutrinos to capture on xenon nuclei. This process, $\text{Xe}(\nu, e^-)\text{Cs}$, is analogous to that employed in the Davis experiment at Homestake. The Feynman diagram for this process results from crossing

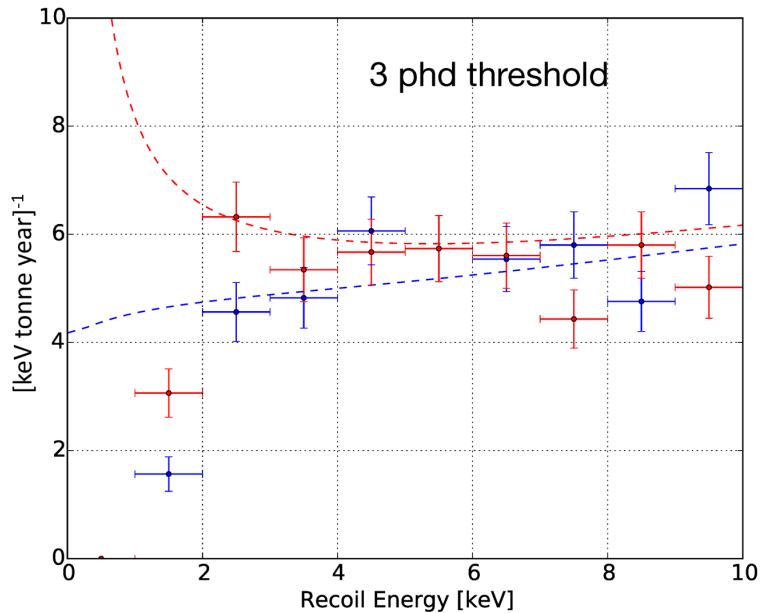


Figure 2.2.2: Predicted neutrino-dominated electron recoil background rate in LZ, for no magnetic moment (blue) and a magnetic moment $5 \times 10^{-12} \mu_B$ (red).

the electron capture process, so we expect the electron capture Q value to set the threshold for neutrino capture proceed. Only ^{131}Xe has a sufficiently low Q value (352 keV) to exhibit sensitivity to the pp neutrinos. A single calculation of the event rate exists [34], from which we estimate <1 events/year in LZ, in the 1.5 keV to 6.5 keV energy window.

The nearest power reactors are about 800 km away, in Fort Calhoun, NE (0.5 GWe), and Cooper, NE (0.8 GWe). The power/distance² distribution shows a broad peak for reactors in Illinois and Wisconsin. The net flux is small enough, however, that we expect negligible detected events from power-reactor neutrinos in LZ.

2.2.2 Double Beta Decay

2.2.2.1 Neutrinoless Double Beta Decay

If the electron neutrino is its own anti-particle, this would allow for the possibility of a process whereby double beta decay occurs but the two neutrinos annihilate. This process is referred to as neutrinoless double beta decay ($0\nu\beta\beta$). In this case, all decay energy goes into the two electrons. Thus, the signature is a mono-energetic, single-site event at the Q-value of the decay. Observation of this process would imply discovery of

1. fermions which are their own anti-particles (so called Majorana particles).
2. Lepton number violation.
3. Violation of conservation of the net difference between baryon and lepton number.

Currently the best lower limit on the half-life for $0\nu\beta\beta$ of ^{136}Xe comes KamLAND-ZEN results, 1.06×10^{26} y [35] at 90 % confidence. Searches involving different xenon isotopes and related processes are discussed in Ref. [36].

Any search for $0\nu\beta\beta$ needs low backgrounds, a large amount of the relevant isotope, and good energy resolution. Note that LZ requirement R-150004 implies a resolution of better than 2.0 % σ/E at 2.5 MeV. The criteria for a $0\nu\beta\beta$ search are very similar to those for a competitive dark matter experiment, however traditionally building an experiment which is competitive for both tends to be quite difficult. The large mass and exceptionally low backgrounds make this search possible in LZ. Typically searches for $0\nu\beta\beta$ use enriched ^{136}Xe to enhance their signal. The 7 tonnes natural xenon implies almost 623 kg of ^{136}Xe , which is more than previous $0\nu\beta\beta$ searches.

The main backgrounds at the ^{136}Xe Q-value are the 2,447.7 keV γ -line from ^{214}Bi in the uranium chain and the 2,614.5 keV γ -line from ^{210}Tl from the thorium chain. Unlike in the many background that are distributed uniformly throughout the active xenon mass in the WIMP-search analysis, these backgrounds are completely from external detector components, and the size of LZ afford substantial screening of these background.

The same background simulations used to estimate the sensitivity of LZ to WIMPs are used to project the sensitivity to $0\nu\beta\beta$. The analysis for $0\nu\beta\beta$ is slightly different because the result is more dependent on the input assumptions. The energy resolution at the Q-value affects the experiment's ability to reject backgrounds from the penetrating 2,614.5 keV ^{210}Tl line. Major background contributions include the TPC PMTs, the xenon vessel, and the resistors. There is some contribution from the radioactivity of the Davis cavern walls that is still under investigation, but at worst some additional shielding may be necessary above and below the xenon vessel, but not on the sides. The sensitivity estimate also depends on the minimal vertex separation needed to identify a multiple scatter and the energy resolution at the Q-value (σ/E). In previous work by [16], it was assumed multiple scatters could be rejected down to 3 mm separations, and we make the same assumption. The choice of fiducial volume for the $0\nu\beta\beta$ search is also different than that for the WIMP

search, because of the penetrating nature of the ^{210}Tl line and the fact that its signal cannot be distinguished by the S1 and S2 signals. Smaller fiducial volumes have less total background due to the self-shielding effect of xenon.

For the purposes of these projections a fiducial volume of 1,000 kg was chosen as a proper tradeoff between backgrounds and exposure. A Feldman-Cousins cut-and-count analysis is used with a 2σ region-of-interest and $Q_{\beta\beta}$. LZ has the potential to a sensitivity to a 90% median expected C.L. limit on the $0\nu\beta\beta$ half-life of ^{136}Xe of 1.2×10^{26} y with an energy resolution (σ/E) of 1.0 % or better. For comparison, at 90 % confidence, the half-life limit from EXO 200 [37] is 1.1×10^{25} y, that from GERDA [38] is 5.3×10^{25} y, and KamLAND-Zen has achieved 1.06×10^{26} y [35].

2.2.2.2 Two Neutrino Double Beta Decay

Two-neutrino double beta decay ($2\nu\beta\beta$) is a standard model decay which has been observed in several isotopes which occurs when single beta decay is energetically forbidden. For example, ^{136}Xe is lighter than ^{136}Cs , so conservation of energy makes single beta decay of ^{136}Xe impossible. However, ^{136}Xe can undergo two simultaneous beta decays, emitting two electrons and two anti-electron neutrinos. This process has been observed in many different isotopes and the half-lives are always greater than 10×10^{18} y.

For example, ^{136}Xe has a half-life due to $2\nu\beta\beta$ of 2.2×10^{21} y [37] and a Q-value of 2,456 keV [39]. LZ should observed 3×10^6 double beta decays over 1,000 live days.

The isotope ^{134}Xe is also believed to undergo $2\nu\beta\beta$ with a Q-value of 826 keV [40].

Although $2\nu\beta\beta$ of ^{136}Xe has been observed by both EXO-200 and KamLAND-ZEN, both had analysis thresholds at or above the peak of the spectrum from $2\nu\beta\beta$ of ^{134}Xe near 800 keV. LZ will be in a position to measure the full spectrum of ^{134}Xe $2\nu\beta\beta$ down to 1 keV_{ee} and see the turnover at the peak of the spectrum.

2.2.3 Supernova Neutrinos

Should a supernova occur in our galaxy during LZ operation, neutrinos emitted from the supernova would be detected via coherent neutrino-nucleus scattering, which is blind with respect to neutrino flavor. The energy spectrum of neutrinos emitted from a typical supernova peaks near 10 MeV, and has a tail that extends above 50 MeV, which causes NRs above the LZ threshold [41]. Coherent neutrino-nucleus scattering is mediated by the weak neutral current, and thus provides important information on the flux and spectrum of muon and tau neutrinos from supernovae, complementary to the signals that would be seen in other detectors. From a supernova in our own galaxy at distance 10 kpc from Earth, LZ would see ~ 50 NR events of energy greater than 6 keV_{nr} in a rapid 10-sec burst [42, 43].

The NR recoil spectrum increases as the recoil energy decreases; a threshold of 3 keV_{nr} would allow detection of ~ 100 supernova neutrino-induced NR events. The current world sample of 19 supernova neutrino-induced events were detected from supernova 1987a, 50 kpc from Earth, by detectors with total mass 1,200 times greater than LZ. A supernova 10 kpc from Earth would cause about 7,000 neutrino-induced events in the 32,000 tonnes of water in the Super-Kamiokande detector [41].

The response of large, liquid xenon detectors to supernova signals has been recently reviewed[44].

2.2.4 Sterile Neutrinos

There are long-standing anomalies arising from the detailed study of antineutrinos from reactors, and from source-calibration of solar neutrino experiments [45]. A recent study has evaluated the capabilities of deployment of a 5 MCi ^{51}Cr electron neutrino source near to the LZ detector [46]. The excellent spatial resolution of the LZ liquid xenon TPC allows the spatial pattern of electron neutrino oscillation into a sterile neutrino

to be detected. A neutrino source experiment with LZ would not be part of the principal LZ science goal, which is the WIMP search, and could constitute a distinct follow-on experiment after the WIMP search had achieved significant results.

The sensitivity achievable by five source deployments of a 5 MCi ^{51}Cr source near LZ is shown in Figure 2.2.3. Numerous proposals are underway to probe the origin of the reactor/source anomalies [47], but the potential LZ advantage is a diminished need to control the source normalization due to LZ's excellent spatial resolution. In addition, a source deployment near LZ will bring sensitivity to an electron neutrino magnetic moment that is close to the limits deduced from astrophysical considerations [46].

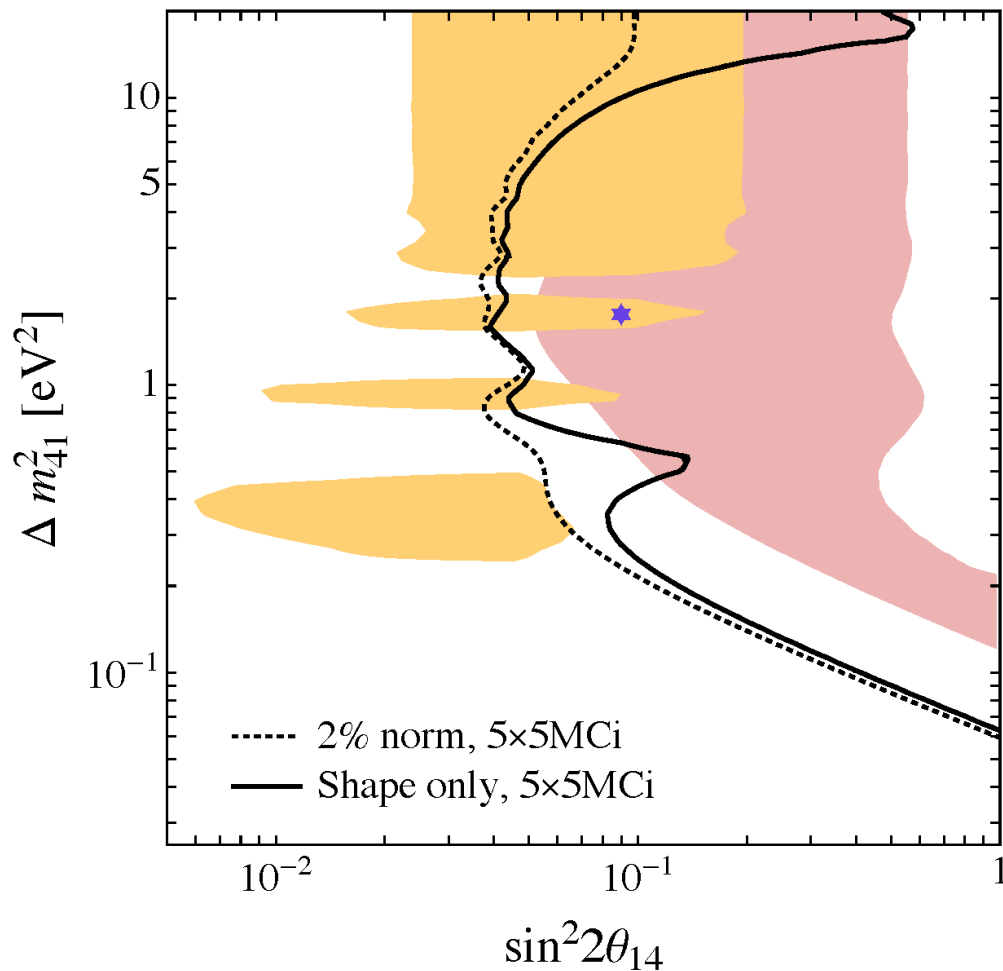


Figure 2.2.3: Sensitivity to sterile neutrino oscillations as a function of mass-difference and mixing angle. The parameter space to the right of each line would be excluded at 95% CL. The shaded areas show the 95% CL allowed regions for source (pink) and reactor (yellow) anomalies. The blue star is the joint best fit. The black solid line shows the expected contours for five 100 d deployments of a 5 MCi ^{51}Cr source next to LZ, without use of the source normalization. The dotted line shows the contour if a 2% normalization of the source is available. From Ref. [46].

2.3 New Physics Beyond Nuclear Recoils from WIMPs

2.3.1 Electrophilic WIMPs

One type of WIMP-matter coupling that does not cause NRs, at least at tree-level, is the coupling of a WIMP to a charged lepton. A WIMP-charged lepton vector coupling induces a WIMP-nucleon interaction at one loop in perturbation theory, where the charged lepton loop interacts with the nucleon via photon exchanges [48]. This interaction is surprisingly sensitive. The WIMP-nucleon SI cross-section sensitivity of $2.3 \times 10^{-48} \text{ cm}^2$ achievable by LZ at a WIMP mass of $40 \text{ GeV}/c^2$ corresponds, when converted via a one-loop calculation, to a WIMP-electron cross section of $1 \times 10^{-50} \text{ cm}^2$. Should the interaction be exclusively WIMP-muon, the LZ sensitivity at $40 \text{ GeV}/c^2$ corresponds to a vector-mediated WIMP-muon cross section of $5 \times 10^{-50} \text{ cm}^2$; for a tau, the corresponding WIMP-tau cross section is $4 \times 10^{-49} \text{ cm}^2$.

If the WIMP is a Majorana particle, all its vector couplings vanish, but an SD axial-vector coupling is still possible. The axial-vector coupling does not induce an interaction at higher order in perturbation theory with the nucleus; the only observable consequence in LZ of an axial-vector coupling of a WIMP to an electron is WIMP-electron scattering.

The electron motion is crucial for the appropriate treatment of WIMP-electron scattering. It is the very highest momentum tails of the electron wavefunction that determine the cross section for an impinging WIMP to ionize a Xe atom. The resulting events are ERs, and their energy spectrum rises very quickly as the energy deposition falls. Limits on axial-vector WIMP-electron scattering depend critically on the low energy threshold [48].

Interpretations of the DAMA [49] event excess as axial-vector WIMP-electron scattering imply a WIMP-electron cross section of $2 \times 10^{-32} \text{ cm}^2$ at a WIMP mass $50 \text{ GeV}/c^2$. The LZ experiment is likely to observe an ER background primarily from ^{219}Rn daughters, about 4 orders of magnitude lower than DAMA backgrounds, so LZ should achieve a limit, assuming background subtraction, of approximately $6 \times 10^{-38} \text{ cm}^2$. This sensitivity is comparable to the indirect astrophysical limits on the SD WIMP-electron scattering cross sections deduced from Super-Kamiokande data [50].

2.3.2 Axions and Axion-like Particles

The axion was introduced to describe the absence of CP-violation in the strong interaction. These particles, known as QCD axions, have a specific relationship between their mass and their coupling to fermions [51–53]. A particle with properties similar to the axion, but without the relationship between mass and fermion coupling, is known as an axion-like particle (ALP) [54].

The LZ experiment will be sensitive to axions and ALPs via the axioelectric effect, where an axion is absorbed and an atomic electron is ejected [55]. In contrast to the photoelectric effect, the mass of the axion or ALP is available for transfer to the atomic electron.

Two sources of axions or ALPs contribute to a possible signal in LZ [56]:

1. Nonrelativistic ALPs that might constitute the dark matter of our galaxy could cause signals in LZ, if their masses are sufficient to provide enough energy to ionize a Xe atom.
2. Axions or ALPs with a mass less than about 15 keV emitted by bremsstrahlung, Compton scattering, or other atomic processes in the sun also can ionize the Xe atoms in LZ [57].

Events caused by axions or ALPs in LZ would be ERs with energy up to a few tens of keV_{ee} . The signal identification relies on the distinct shape of the energy spectrum of the axion or ALP signal.

The signal for a galactic dark-matter ALP would be a peak in ERs with energy at the mass of the particle. Our studies indicate that the LZ sensitivity to the coupling between electrons and galactic dark-matter ALPs

ranges from a coupling constant g_{Ae} of 10^{-14} to one of 10^{-13} for masses between $1 \text{ keV}/c^2$ and $20 \text{ keV}/c^2$, as shown in Figure 2.3.1.

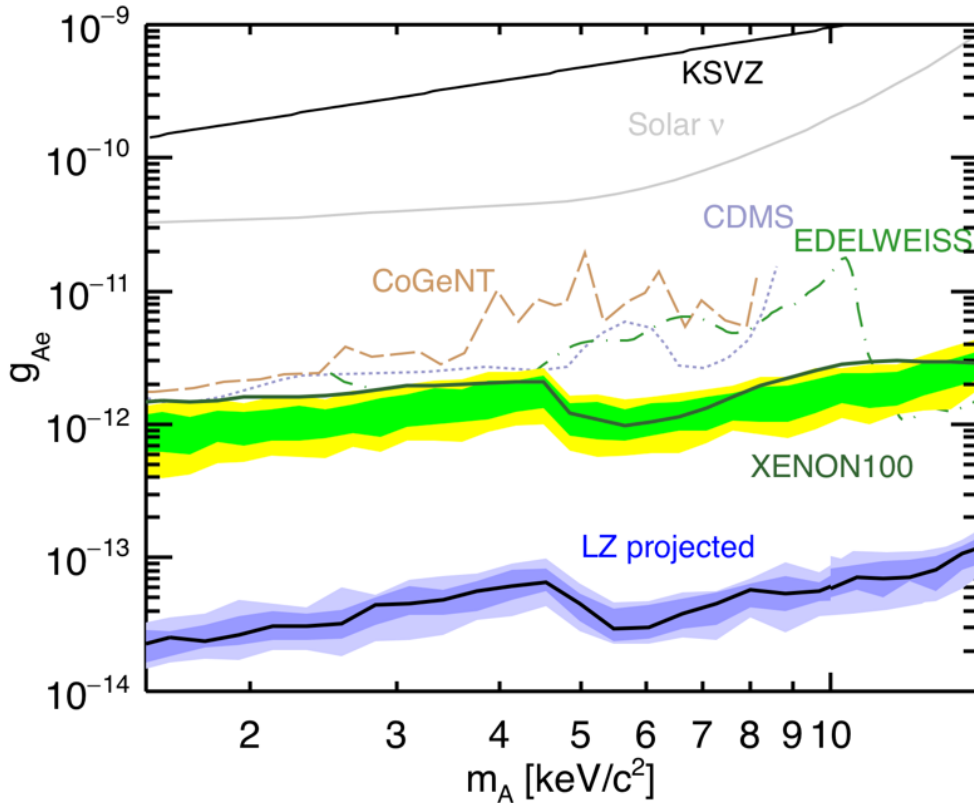


Figure 2.3.1: Dark-matter axion-like particle sensitivity. The LZ projected sensitivity for ALPs at 90 % CL is shown by the dark/light blue bands, which show the 68 % (1σ) and 95 % (2σ) bands for that sensitivity. The line that defines KSVZ axions [58, 59], an astrophysical upper limit from solar neutrinos [60], is shown. Upper limits by the experiments CDMS [61], EDELWEISS [62], CoGeNT [63], and XENON100 [64] are also shown.

The signal for solar ALPs is a broad thermal spectrum caused principally by bremsstrahlung and the Compton effect in the sun convolved with the axioelectric cross section. Our studies indicate that LZ is sensitive to a coupling constant g_{Ae} between solar ALPs and the electron of about 1.3×10^{-12} for masses between $0 \text{ keV}/c^2$ and approximately $1 \text{ keV}/c^2$, as shown in Figure 2.3.2.

2.4 Physics with the Outer Detector

The primary goal of the LZ Outer Detector (OD) consisting of Gd-loaded liquid scintillator (approximately 20t) surrounded by water is to efficiently veto events in the LXe TPC which have additional energy depositions in the OD. These events are background to the WIMP search. However, the OD could be used for additional physics analyses on its own or together with the LXe. A better understanding of possible background induced by muons requires dedicated studies with the OD. The OD is also sensitive to neutrino and weak signals from exotic particles which are dark matter candidates.

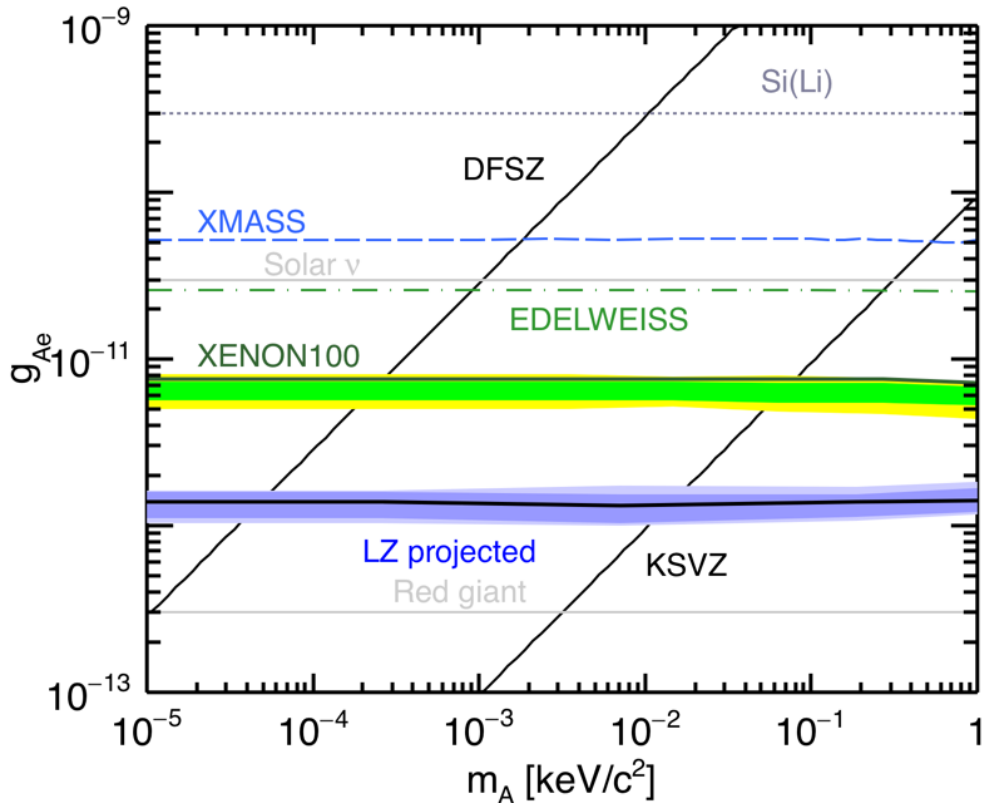


Figure 2.3.2: Solar axion-like particle sensitivity. Horizontal lines all extend down to $m_A = 0$. The LZ projected sensitivity for ALPs at 90% CL is shown by the dark/light blue bands, which show the 68% (1σ) and 95% (2σ) bands for that sensitivity. The lines that define DFSZ axions [65, 66] and KSVZ axions [58, 59], neutrinos [60], and from red giants [67], are shown. Upper limits by the experiments XMASS [68], EDELWEISS [62], and XENON100 [64] are also shown.

2.4.1 Muons and muon-induced neutrons

A few potential physics topics to be addressed by the OD of LZ are linked to muons and muon-induced neutrons. The muon flux at the Davis Campus at SURF has been calculated as $6.2 \times 10^{-5} \text{ m}^{-2} \text{ s}^{-1}$, giving the muon event rate in the OD (water Cherenkov plus liquid organic scintillator) of about 300 per day. Most of these events will be single muons with multiple muons contributing a small fraction ($<1\%$).

There will also be a few hundred of stopping muons detected in scintillator and/or LXe in 1,000 days of running time. Stopping muons can be identified by a delayed signal from either muon decay or absorption on a nucleus LZ will be able to measure the rate of stopping muon signals and the life-time of muons, although no separation between positive and negative muons is possible, apart from detecting neutron capture from absorption of negative muons.

The high probability of neutron detection in the OD having a delayed coincidence with a muon signal allows the identification of a negative muon absorption. Nuclear recoils in LXe will be delayed by a few microseconds with respect to the muon ionization signal, providing a measurements of the negative muon life time in xenon. These measurements require operation of the OD and LXe in coincidence and an independent trigger from the OD.

The detection of neutron capture events will also allow the measurements of neutron yields from this specific process. The accurate interpretation of the results will require the full Monte Carlo simulations of all processes involved including detector response.

Probably the most important measurements that can be carried out by the OD (also in combination with LXe target) are muon-induced neutrons. There have been a number of measurements of neutron production by muons including muon-induced cascades, come carried out by the dark matter search experiments. [69–71]

Neutrons are usually identified via their capture on hydrogen or other elements (for instance, Gd) in active veto systems containing a liquid organic scintillator. With a very large OD (water and scintillator), LZ will detect many thousands of neutrons within its expected 1,000 days of running time. These neutron events will be efficiently rejected in dark matter analysis using various cuts but can be studied for the purpose of better understanding their production, transport and detection. This is particularly important for designing 3rd generation dark matter experiments, especially if a dark matter signal is found, as well as for other rare event searches.

In a conventional analysis, the muon trigger can be provided by either the LXe target or the OD system, and neutrons can be produced in a number of materials in the LZ setup (xenon, titanium, steel, scintillator, water), moderated by hydrogen in scintillator or water and captured predominantly on Gd (or hydrogen) in scintillator.

In addition, with a large mass of LXe, we expect to have hundreds of events with NRs without a muon in LXe allowing studies of NR rate, multiplicities and separation from primary muons (also in delayed coincidences with neutron capture signals).

2.4.2 Neutrinos

The possible sources of neutrino signals in the LZ OD include solar neutrinos, geoneutrinos, supernova bursts and neutrinos from LBNF. In general the LZ OD is not competitive with dedicated neutrino detectors due to its small mass. The supernova burst similar to the SN1987A would give approximately 10 events in the OD. The rate of geoneutrinos is approximately 1 per year. Our estimates of signals from the LBNF neutrinos give 9 events per year for the low energy beam and 25 events per year for the medium energy beam.

2.4.3 Exotic particles

Models of the exotic candidates to be the dark matter include the ones where an excitation can happen in the LXe and deexcitation in the OD. The standard approach would veto such events. A method to discover such interactions would be to measure the spectrum of energy depositions in the OD as it is expected that it should be monochromatic. Another exotic candidate for DM is a fractionally charged particle. The OD could be sensitive to particles with charges down to a fraction of 0.025 of the elementary charge, and coincidences with the LXe TPC provide an interesting cross check. Given the relatively large mass, quietness of the detector, and long exposure time the OD can contribute important capability to these searches.

2.5 Bibliography

- [1] D. S. Akerib *et al.* (LUX), “Low-energy (0.7-74 keV) nuclear recoil calibration of the LUX dark matter experiment using D-D neutron scattering kinematics,” (2016), submitted to *Phys. Rev. C*, [arXiv:1608.05381](https://arxiv.org/abs/1608.05381) [physics.ins-det].
- [2] D. S. Akerib *et al.* (LUX), *Phys. Rev.* **D93**, 072009 (2016), [arXiv:1512.03133](https://arxiv.org/abs/1512.03133) [physics.ins-det].

- [3] M. Pato, L. E. Strigari, R. Trotta, and G. Bertone, *J. Cosmol. Astropart. Phys.* **2013**, 041 (2013), [arXiv:1211.7063 \[astro-ph\]](#).
- [4] D. S. Akerib *et al.* (LUX), *Phys. Rev. Lett.* **116**, 161301 (2016), [arXiv:1512.03506 \[astro-ph\]](#).
- [5] D. S. Akerib *et al.* (LUX), *Phys. Rev. Lett.* **118**, 021303 (2017), [arXiv:1608.07648 \[astro-ph.CO\]](#).
- [6] R. Barbieri, M. Frigeni, and G. F. Giudice, *Nucl. Phys.* **B313**, 725 (1989).
- [7] M. A. Shifman, A. I. Vainshtein, and V. I. Zakharov, *Phys. Lett.* **B78**, 443 (1978).
- [8] J. D. Lewin and P. F. Smith, *Astropart. Phys.* **6**, 87 (1996).
- [9] C. McCabe, *Phys. Rev.* **D82**, 023530 (2010), [arXiv:1005.0579 \[hep-ph\]](#).
- [10] D. S. Akerib *et al.* (LZ), (2015), Conceptual Design Report; LBNL-190005, FERMILAB-TM-2621-AE-E-PPD, [arXiv:1509.02910 \[physics.ins-det\]](#).
- [11] G. Cowan, K. Cranmer, E. Gross, and O. Vitells, *Eur. Phys. J.* **C71**, 1554 (2011), [Erratum: *Eur. Phys. J.* **C73**, 2501 (2013)], [arXiv:1007.1727 \[physics.data-an\]](#).
- [12] P. Sorensen *et al.*, in *Proceedings, 8th International Workshop on The Identification of Dark Matter (IDM 2010)*, Proc. of Science, Vol. **IDM2010** (2011) p. 017, *Lowering the low-energy threshold of xenon detectors*, [arXiv:1011.6439 \[astro-ph\]](#).
- [13] C. McCabe, (2017), [arXiv:1702.04730 \[hep-ph\]](#).
- [14] J. Billard, L. Strigari, and E. Figueroa-Feliciano, *Phys. Rev.* **D89**, 023524 (2014), [arXiv:1307.5458 \[hep-ph\]](#); F. Ruppin, J. Billard, E. Figueroa-Feliciano, and L. Strigari, *Phys. Rev.* **D90**, 083510 (2014), [arXiv:1408.3581 \[hep-ph\]](#).
- [15] J. N. Bahcall and C. Peña-Garay, *New J. Phys.* **6**, 63 (2004), [arXiv:hep-ph/0404061 \[hep-ph\]](#).
- [16] L. Baudis, A. Ferella, A. Kish, A. Manalaysay, T. Marrodan Undagoitia, and M. Schumann, *J. Cosmol. Astropart. Phys.* **2014**, 044 (2014), [arXiv:1309.7024 \[physics.ins-det\]](#).
- [17] J. Beringer *et al.* (Particle Data Group), *Phys. Rev.* **D86**, 010001 (2012).
- [18] W. C. Haxton, R. G. Hamish Robertson, and A. M. Serenelli, *Ann. Rev. Astron. Astrophys.* **51**, 21 (2013), [arXiv:1208.5723 \[astro-ph\]](#).
- [19] J.-W. Chen, H.-C. Chi, C. P. Liu, and C.-P. Wu, (2016), [arXiv:1610.04177 \[hep-ex\]](#); V. L. Morgunov and I. O. Pilugin, “Low-energy neutrino weak and electromagnetic scattering cross-sections on atomic electrons,” (1996), [ITEP-28-96](#).
- [20] J. N. Abdurashitov *et al.* (SAGE), *Phys. Rev.* **C80**, 015807 (2009), [arXiv:0901.2200 \[nucl-ex\]](#).
- [21] G. Bellini *et al.* (Borexino), *Nature* **512**, 383 (2014).
- [22] D. Z. Freedman, *Phys. Rev.* **D9**, 1389 (1974).
- [23] B. Cabrera, L. M. Krauss, and F. Wilczek, *Phys. Rev. Lett.* **55**, 25 (1985).
- [24] L. E. Strigari, *New J. Phys.* **11**, 105011 (2009), [arXiv:0903.3630 \[astro-ph\]](#).

- [25] B. Aharmim *et al.* (SNO), *Phys. Rev.* **C88**, 025501 (2013), arXiv:1109.0763 [nucl-ex].
- [26] G. Battistoni, A. Ferrari, T. Montaruli, and P. R. Sala, *Astropart. Phys.* **23**, 526 (2005).
- [27] D. Smart and M. Shea, *Adv. Space Res.* **36**, 2012 (2005), solar Wind-Magnetosphere-Ionosphere Dynamics and Radiation Models.
- [28] C. Arpesella *et al.* (Borexino), *Phys. Rev. Lett.* **101**, 091302 (2008), arXiv:0805.3843 [astro-ph].
- [29] J. M. Lattimer and J. Cooperstein, *Phys. Rev. Lett.* **61**, 23 (1988).
- [30] E. Sanshiro, *Neutrino Geophysics and Observation of Geo-Neutrinos at KamLAND*, Ph.D. thesis, Tohoku University (2005).
- [31] T. Araki *et al.*, *Nature* **436**, 499 (2005).
- [32] S. Enomoto, E. Ohtani, K. Inoue, and A. Suzuki, *Earth Planet. Sc. Lett.* **258**, 147 (2007).
- [33] G. Bellini *et al.* (Borexino), *Phys. Lett.* **B687**, 299 (2010), arXiv:1003.0284 [hep-ex].
- [34] A. S. Georgadze, H. V. Klapdor-Kleingrothaus, H. Pas, and Yu. G. Zdesenko, *4th International Solar Neutrino Conference Heidelberg, Germany, April 8-11, 1997*, *Astropart. Phys.* **7**, 173 (1997), [283(1997)], arXiv:nucl-ex/9707006 [nucl-ex].
- [35] A. Gando *et al.* (KamLAND-Zen), *Phys. Rev. Lett.* **117**, 082503 (2016), [Addendum: *Phys. Rev. Lett.* 117,no.10,109903(2016)], arXiv:1605.02889 [hep-ex].
- [36] N. Barros, J. Thurn, and K. Zuber, *J. Phys.* **G41**, 115105 (2014), arXiv:1409.8308 [nucl-ex].
- [37] J. B. Albert *et al.* (EXO-200), *Nature* **510**, 229 (2014), arXiv:1402.6956 [nucl-ex].
- [38] M. Agostini *et al.* (GERDA), (2017), arXiv:1703.00570 [nucl-ex].
- [39] M. Redshaw, E. Wingfield, J. McDaniel, and E. G. Myers, *Phys. Rev. Lett.* **98**, 053003 (2007).
- [40] M. Wang, G. Audi, A. Wapstra, F. Kondev, M. MacCormick, X. Xu, and B. Pfeiffer, *Chin. Phys.* **C36**, 1603 (2012).
- [41] K. Scholberg, *Ann. Rev. Nucl. Part. Sci.* **62**, 81 (2012), arXiv:1205.6003 [astro-ph].
- [42] C. J. Horowitz, K. J. Coakley, and D. N. McKinsey, *Phys. Rev.* **D68**, 023005 (2003), arXiv:astro-ph/0302071 [astro-ph].
- [43] S. Chakraborty, P. Bhattacharjee, and K. Kar, *Phys. Rev.* **D89**, 013011 (2014), arXiv:1309.4492 [astro-ph].
- [44] R. F. Lang, C. McCabe, S. Reichard, M. Selvi, and I. Tamborra, *Phys. Rev.* **D94**, 103009 (2016), arXiv:1606.09243 [astro-ph.HE].
- [45] K. N. Abazajian *et al.*, “Light Sterile Neutrinos: A White Paper,” (2012), (unpublished), arXiv:1204.5379 [hep-ph].
- [46] P. Coloma, P. Huber, and J. M. Link, *J. High Energy Phys. (online)* **2014**, 042 (2014), arXiv:1406.4914 [hep-ph].

- [47] B. Caccianiga, in *XXVI INTERNATIONAL CONFERENCE ON NEUTRINO PHYSICS AND ASTROPHYSICS: Neutrino 2014*, AIP Conf. Proc., Vol. 1666 (2015) p. 180002, *Future short baseline neutrino searches with nuclear decays*; D. Lhuillier, in *XXVI INTERNATIONAL CONFERENCE ON NEUTRINO PHYSICS AND ASTROPHYSICS: Neutrino 2014*, Vol. 1666 (2015) p. 180003, *Future short-baseline sterile neutrino searches with reactors*.
- [48] J. Kopp, V. Niro, T. Schwetz, and J. Zupan, *Phys. Rev.* **D80**, 083502 (2009), arXiv:0907.3159 [hep-ph].
- [49] R. Bernabei *et al.* (DAMA), *Nuclear Physics in Astrophysics. Proceedings, 17th International Conference, NPDC 17, Debrecen, Hungary, September 30 to October 4, 2002*, *Nucl. Phys.* **A719**, 257 (2003), *Searching for the dark universe by the DAMA experiment*.
- [50] T. Tanaka *et al.* (Super-Kamiokande), *Astrophys. J.* **742**, 78 (2011), arXiv:1108.3384 [astro-ph].
- [51] R. D. Peccei and H. R. Quinn, *Phys. Rev. Lett.* **38**, 1440 (1977).
- [52] S. Weinberg, *Phys. Rev. Lett.* **40**, 223 (1978).
- [53] F. Wilczek, *Phys. Rev. Lett.* **40**, 279 (1978).
- [54] K. A. Olive *et al.* (Particle Data Group), *Chin. Phys.* **C38**, 090001 (2014), Review of Particle Physics: *Gauge and Higgs Bosons*, A. Ringwald, L.J Rosenberg, and G. Rybka, *Axions and Other Similar Particles*, pp. 626-635.; J. Beringer *et al.* (Particle Data Group), *Phys. Rev. D* **86**, 010001 (2012).
- [55] S. Dimopoulos, G. D. Starkman, and B. W. Lynn, *Phys. Lett.* **B168**, 145 (1986).
- [56] K. Arisaka, P. Beltrame, C. Ghag, J. Kaidi, K. Lung, A. Lyashenko, R. D. Peccei, P. Smith, and K. Ye, *Astropart. Phys.* **44**, 59 (2013), arXiv:1209.3810 [astro-ph].
- [57] J. Redondo, *J. Cosmol. Astropart. Phys.* **2013**, 008 (2013), arXiv:1310.0823 [hep-ph].
- [58] J. E. Kim, *Phys. Rev. Lett.* **43**, 103 (1979).
- [59] M. A. Shifman, A. I. Vainshtein, and V. I. Zakharov, *Nucl. Phys.* **B166**, 493 (1980).
- [60] P. Gondolo and G. Raffelt, *Phys. Rev.* **D79**, 107301 (2009), arXiv:0807.2926 [astro-ph].
- [61] Z. Ahmed *et al.* (CDMS-II), *Phys. Rev. Lett.* **103**, 141802 (2009), arXiv:0902.4693 [hep-ex].
- [62] E. Armengaud *et al.* (EDELWEISS-II), *J. Cosmol. Astropart. Phys.* **2013**, 067 (2013), arXiv:1307.1488 [astro-ph].
- [63] C. E. Aalseth *et al.* (CoGeNT), *Phys. Rev. Lett.* **101**, 251301 (2008), [Erratum: *Phys. Rev. Lett.* **102**, 109903 (2009)], arXiv:0807.0879 [astro-ph].
- [64] E. Aprile *et al.* (XENON100), *Phys. Rev.* **D90**, 062009 (2014), arXiv:1404.1455 [astro-ph].
- [65] A. R. Zhitnitsky, *Sov. J. Nucl. Phys.* **31**, 260 (1980), [*Yad. Fiz.* **31**, 497 (1980)].
- [66] M. Dine, W. Fischler, and M. Srednicki, *Phys. Lett.* **B104**, 199 (1981).
- [67] G. G. Raffelt, in *Axions: Theory, Cosmology, and Experimental Searches, Proceedings, 1st Joint ILIAS-CERN-CAST Axion Training, Geneva, Switzerland, November 30-December 2, 2005*, *Lect. Notes Phys.*, Vol. **741** (2008) pp. 51–71, *Astrophysical Axion Bounds*, arXiv:hep-ph/0611350 [hep-ph].

- [68] K. Abe *et al.* (XMASS), *Phys. Lett.* **B724**, 46 (2013), arXiv:1212.6153 [astro-ph].
- [69] H. M. Araujo *et al.*, *Astropart. Phys.* **29**, 471 (2008), arXiv:0805.3110 [hep-ex].
- [70] L. Reichhart *et al.* (ZEPLIN-III), *Astropart. Phys.* **47**, 67 (2013), arXiv:1302.4275 [physics.ins-det].
- [71] B. Schmidt *et al.* (EDELWEISS), *Astropart. Phys.* **44**, 28 (2013), arXiv:1302.7112 [astro-ph.CO].